

GSA DATA REPOSITORY 2016175

Recent volcanic resurfacing of Venusian craters

Jennifer L. Whitten¹, and Bruce A. Campbell¹

¹Center for Earth and Planetary Studies, Smithsonian Institution, MRC 315, PO Box 37012, Washington, DC 20013-7012, United States.

Data Repository

Contents of this file

Supplemental text:

Parabolic ejecta deposit volumes

Eruption rates at Sudenitsa Tesserae

Supplemental Figures DR 1, DR 2, and DR 3

Supplemental Tables 1 and 2

METHODS

Calculation of parabolic ejecta deposit volumes

Volumes of the observed parabolic ejecta deposits were determined based on the measured area of the radar-dark backslopes visible in the Magellan dataset. Areas of $2.4 \times 10^5 \text{ km}^2$, $2.6 \times 10^5 \text{ km}^2$, and $\sim 1.7 \times 10^5 \text{ km}^2$ were calculated for radar-dark backslope regions at Alpha, Tellus, and Sudenitsa tesserae, respectively (Table DR1). These area values were then multiplied by a thickness estimate of 10 cm (see Campbell et al., 1992; Schaller and Melosh, 1998; Campbell et al., 2015). Volumes of the observed radar-dark material at Alpha, Tellus, and Sudenitsa are thus 24 km^3 , 26 km^3 , and $\sim 17 \text{ km}^3$ which is only a small fraction of the total volume of ejecta produced during these impact events (Table DR1). Total crater volume and ejecta volume were calculated using the method of Basilevsky et al. (2004); crater volume was estimated using a cylindrical cavity shape and ejecta volume was assumed to be half of the crater volume. These deposit volumes represent only a fraction of the total parabolic ejecta deposit, because the areas only include regions of radar-dark materials detected using Magellan SAR data. Regardless, these calculated volumes are consistent with previous parabolic ejecta deposit estimates (Basilevsky et al., 2004).

Calculation of eruption rates at Sudenitsa Tessera

Eruption rates were estimated from the areal coverage of preserved ejecta material at Sudenitsa Tesserae; the length ($\sim 1155 \text{ km}$) and width ($\sim 1275 \text{ km}$) of the radar-dark band of tesserae at 260°E was used to estimate the size of a parabolic deposit and the location and size of the source crater (Supplementary Table 1; Fig. 3). These measurements were used to calculate other morphologic characteristics of the parabolic ejecta deposits based on linear relationships between the different variables defined by (Schaller and Melosh, 1998, their Fig. 3), including

the maximum width of the fine-grained ejecta deposit (W_{\max}), the width at the center longitude of the source crater (W_c), the total length of the fine-grained parabolic deposit (L_T), and the distance between the center of the source crater and the easternmost extent of the fine-grained materials (L_c).

The length of the radar-dark region was assumed to be either W_c or W_{\max} , resulting in two possible parabolic ejecta deposit shapes (Fig. 3b, c; Table DR1 rows 3 and 4). These variables can also be used to determine the source crater diameter and location (Fig. 3d; Supplementary Table 1); at Sudenitsa the source crater is between 20 and 30 km in diameter. Predicted source crater diameters were then used to determine the approximate rim height of a fresh crater using morphometric relationships from (Herrick and Sharpton, 2000) for bright-floored impact craters >15 km in diameter, giving a range in rim height from 0.05 to 0.83 km.

Two separate resurfacing scenarios for Sudenitsa are proposed in the text: (1) the fine-grained ejecta and the source crater were completely resurfaced by volcanic flows, and (2) the fine-grained parabola material on the plains was eroded by aeolian processes and the source crater was removed by volcanic flows. For scenario 1, the areas of the two hypothetical parabolic ejecta deposits (Fig. 3b, c) confined to regional plains materials ($1.1 \times 10^6 \text{ km}^2$ and $1.5 \times 10^6 \text{ km}^2$) were multiplied by the rim height estimates to determine the volume of volcanic material required to completely remove the crater and the fine-grained ejecta, 5.4×10^4 – $1.2 \times 10^6 \text{ km}^3$; an average lava volume for each parabola size would be $2.5 \times 10^5 \text{ km}^3$ and $3.5 \times 10^5 \text{ km}^3$, respectively. The estimated flow areas are consistent with large lava flow fields on Venus, such as Mylitta Fluctus ($3.0 \times 10^5 \text{ km}^2$) and the field near Ozza Mons ($1.8 \times 10^5 \text{ km}^2$) (Head et al., 1992), and Large Igneous Provinces on Earth (e.g., Ontong Java: $5 \times 10^6 \text{ km}^2$ and $6 \times 10^7 \text{ km}^2$) (Coffin and Eldholm, 1993). Lunar mare deposits within large impact basins, such as Mare Serenitatis have comparable areas and volumes, $3.5 \times 10^6 \text{ km}^2$ (Whitford-Stark, 1982) and $5 \times 10^5 \text{ km}^3$ (Hackwill, 2010). These comparisons suggest that the calculated values for Venus are reasonable.

These two average volumes were divided by the average calculated age of the parabolic ejecta deposits (35 Ma, Schaller and Melosh, 1998), plus 3σ , to estimate eruption rates. We assume the additional 3σ to account for the potential age difference between the preservation of fine-grained ejecta in the plains and highly deformed tessera terrains. These volume and age values yield average eruption rates of $3.1 \times 10^{-3} \text{ km}^3/\text{yr}$ and $4.4 \times 10^{-3} \text{ km}^3/\text{yr}$. However, based

on the variability of the rim height and area estimates, eruption rates could fall between 7×10^{-4} and $2 \times 10^{-2} \text{ km}^3/\text{yr}$.

For the second scenario, where only the source crater is removed by volcanic flows (and the radar-dark parabolic ejecta is removed by aeolian processes), the areal extent of a small eruption event required to completely cover the source crater and its proximal ejecta out to 3 crater radii (Phillips et al., 1991) is between $2.8 \times 10^3 \text{ km}^2$ to $6.4 \times 10^3 \text{ km}^2$, with an average value of $4.4 \times 10^3 \text{ km}^2$. Using the same crater rim heights from scenario 1 results in an average volume of $1.0 \times 10^3 \text{ km}^3$ (and a range between $1.4 \times 10^2 \text{ km}^3$ and $5.3 \times 10^3 \text{ km}^3$). This much smaller eruption results in an average eruption rate of $1.3 \times 10^{-5} \text{ km}^3/\text{yr}$ over 80 Ma. However, it is unlikely that such a small eruption lasted for 80 Ma, so assuming a more reasonable duration of 8 Ma results in an average eruption rate of $1.3 \times 10^{-4} \text{ km}^3/\text{yr}$ (with a range between $1.8 \times 10^{-5} \text{ km}^3/\text{yr}$ and $6.6 \times 10^{-4} \text{ km}^3/\text{yr}$).

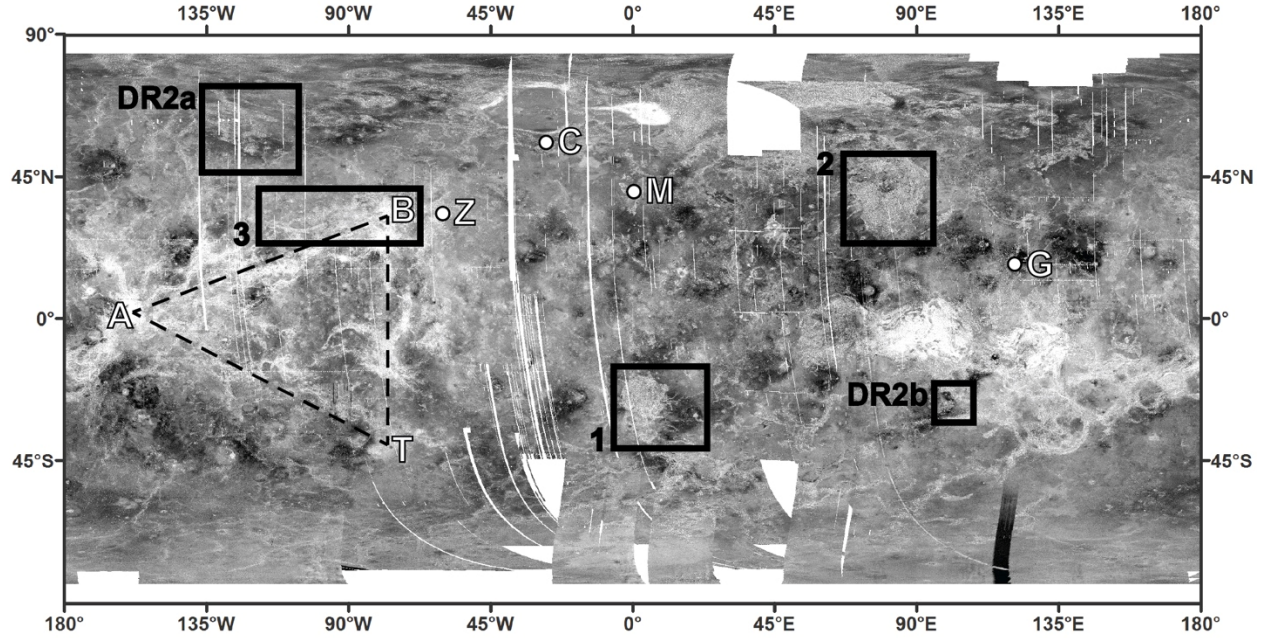


Figure DR1. Location of geologic features and regions discussed in the text. Labeled black boxes mark the location of figures in the main (1- Alpha Regio, 2-Tellus Tessera, 3-Sudenitsa Tesserae) and supplementary (DR2a, DR2b) text. Dashed black triangle denotes the location of the Beta-Atla-Themis (BAT) region which has a high density of volcanic features and a relatively low density of impact craters (see text for more details). The white circles and associated letters Z, C, M and G mark the location of Zirka, Clotho, Manzan-Gurme, and Gegute tesserae, respectively.

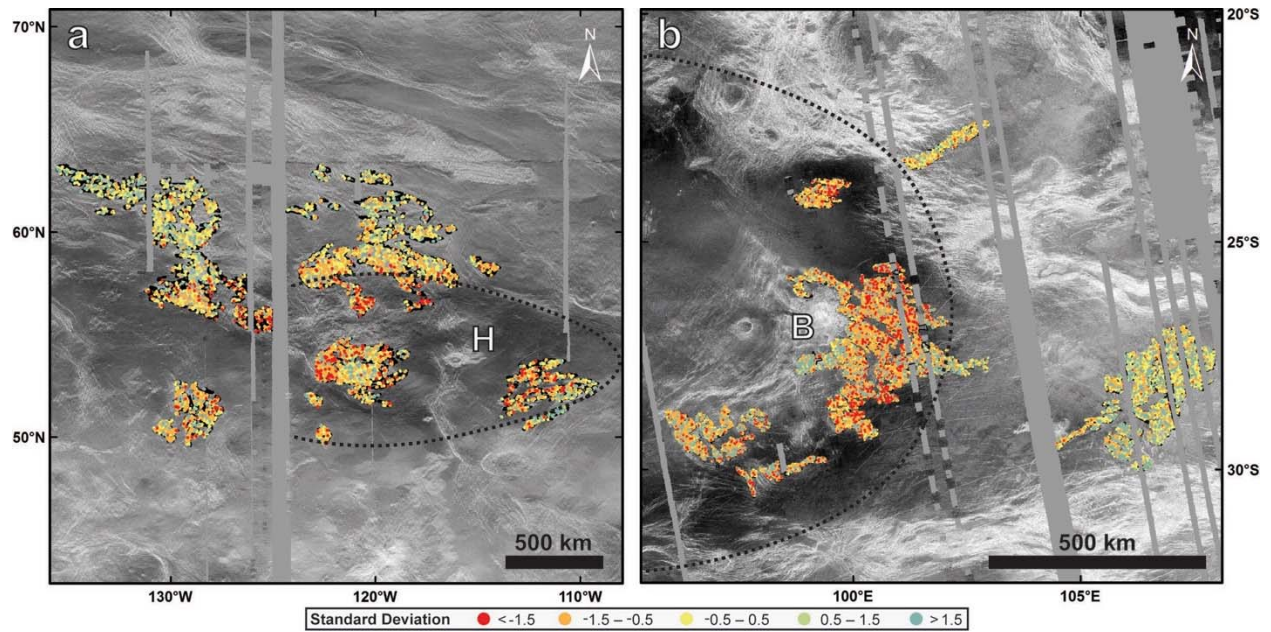


Figure DR2. Evidence for positive detection of fine-grained, parabolic ejecta deposits in tesserae. (a) Virilis Tesserae and known parabolic ejecta crater Hayashi (H; 43.1 km in diameter). Dashed black line represents the measured parabolic ejecta deposit boundary as reported in (Schaller and Melosh, 1998). Dots are color-coded by the standard deviation of the backscatter coefficient value, where the darkest materials are shown in red, and the brightest materials in blue (applies to dots in panel b). There is a distinct shift in the radar brightness of backslopes in the northern extent of Virilis Tesserae that defines the northern boundary of the parabolic ejecta deposit. (b) Husbishag Tessera and Boulanger crater (B; 71.5 km in diameter) with its associated parabolic ejecta deposit. There is a sharp change in the radar brightness of backslopes inside (west of the black dashed line) and outside (east of the black dashed line) of the parabolic ejecta deposit.

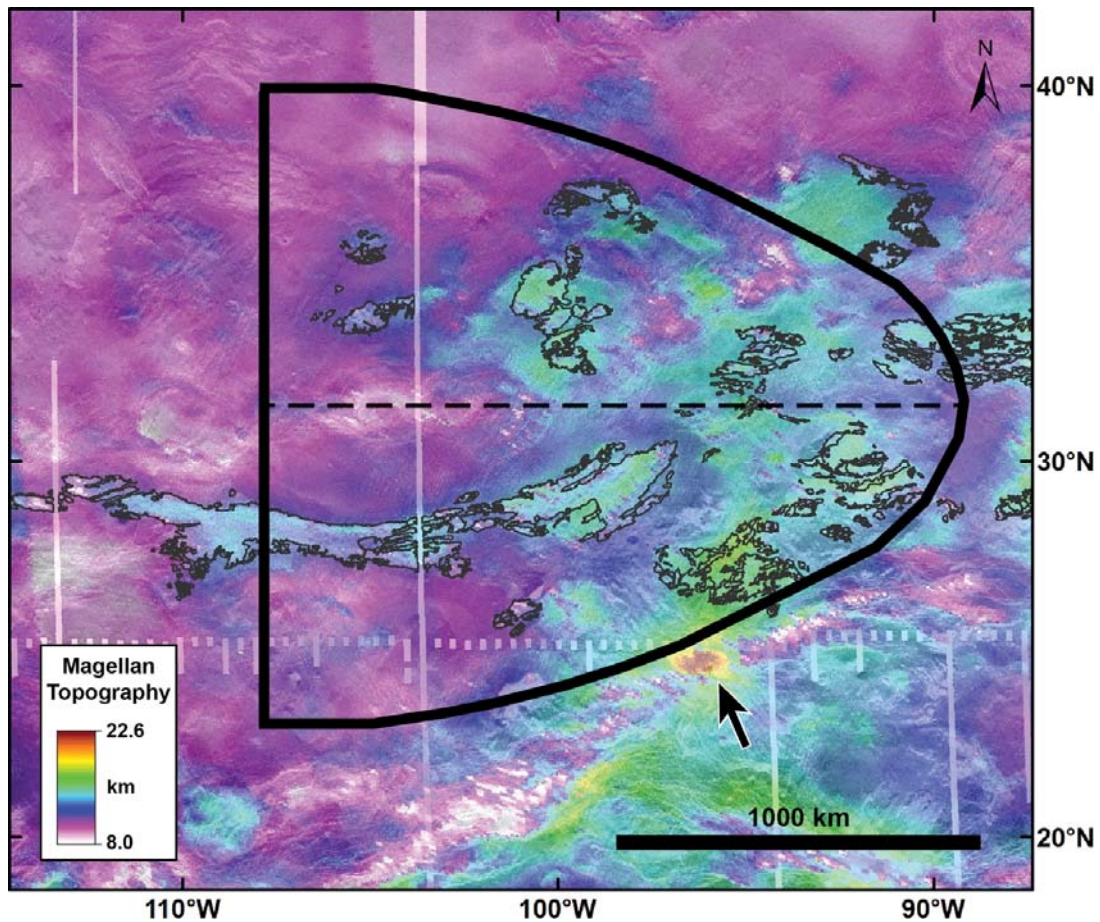


Figure DR3. Elevations of the Sudenitsa Tessera region. Black parabola represents the potential location of the original parabolic ejecta deposit and dashed horizontal line is the approximate latitude of the source crater. The source crater is predicted to be on the right side of the parabola, though there are no obvious depressions or elevated rims to indicate a buried crater. Arrow indicates the location of Polik-mana Mons (600 km diameter volcano), a potential source of lavas that buried the source crater of the radar-dark material preserved in the Sudenitsa tessera. Magellan left-look SAR overlain with Magellan topography (4.6 km/ pixel).

Table DR1. Crater, ejecta, and radar-dark material volume estimates.¹

Crater Diameter (km)	Depth (km ²)	Crater Volume (km ³)	Ejecta Volume (km ³)	Parabola Area (km ²)	Vol. 5-cm parabola (km ³)	Fraction of crater vol.	Fraction of ejecta vol.
Stuart, 69 km	1.42	5327	2664	2.9E+06	145	0.027	0.054
Stuart, radar-dark tessera Earth	-	-	-	4.2E+05	21	0.004	0.008
Stuart, radar-dark tessera Magellan	-	-	-	2.4E+05	12	0.002	0.004
Bernhardt, 25 km	1.05	516	258	4.6E+05	23	0.045	0.089
Bernhardt, radar-dark tessera	-	-	-	2.6E+05	13	0.025	0.049
Sudenitsa, 20 km	0.98	309	154	1.2E+06	60	0.194	0.389
20 km, radar-dark	-	-	-	1.5E+05	8	0.024	0.049
Sudenitsa, 30 km	1.11	784	392	1.7E+06	84	0.107	0.214
30 km, radar-dark	-	-	-	1.8E+05	9	0.012	0.024

¹See “Methods: Calculation of parabolic ejecta volumes” above for more detail.

Table DR2. Calculated parabolic ejecta deposit fit variables^a.

Name	Radius (km)^b	L_c (km)^c	W_c (km)^d	L_T (km)^e	W_{max} (km)^f
Bernhardt crater	12.7	138	436	756	774
Sudenitsa "source crater"	22.6	266	803	1154^f	1202
	23.3	267	835	1138	1276^g
	32.5	435	1276^g	1369	1526

^aVariables defined in Schaller and Melosh (1998).

^bRadius of hypothetical source crater.

^cDistance from the center of the source crater to the eastern edge of the parabolic ejecta deposit.

^dWidth of the parabolic ejecta deposit at the center longitude of the source crater.

^eTotal length of the parabolic ejecta deposit.

^fMaximum width of the parabolic ejecta deposit.

^gMeasurements of the dark backslope region in Sudenitsa Tesserae used to estimate the size and location of both the source crater and the parabolic ejecta deposit.

References

- Basilevsky, A.T., Head, J.W., Abdrakhimov, A.M., 2004, Impact crater air fall deposits on the surface of Venus: Areal distribution, estimated thickness, recognition in surface panoramas, and implications for provenance of sampled surface materials: *Journal of Geophysical Research*, v. 109, p. E12003, doi:10.1029/2004JE002307.
- Coffin, M.F., Eldholm, O., 1993, Scratching the surface: Estimating dimensions of large igneous provinces: *Geology*, v. 21, p. 515–518.
- Hackwill, T., 2010, Stratigraphy, evolution, and volume of basalts in Mare Serenitatis: *Meteoritics and Planetary Science*, v. 45, p. 210–219, doi:10.1111/j.1945-5100.2010.01018.x.

- Herrick, R.R., and Sharpton, V.L., 2000, Implications from stereo-derived topography of Venusian impact craters: *Journal of Geophysical Research*, v. 105, p. 20245–20262, doi:10.1029/1999JE001225.
- Phillips, R.J., Arvidson, R.E., Boyce, J.M., Campbell, D.B., Guest, J.E., Schaber, G.G., Soderblom, L.A., 1991, Impact craters on Venus: Initial analysis from Magellan: *Science*, v. 252, p. 288–297, doi:10.1126/science.252.5003.288.
- Schaller, C.J., and Melosh, H.J., 1998, Venusian ejecta parabolas: Comparing theory with observations: *Icarus*, v. 131, p. 123–137, doi:10.1006/icar.1997.5855.
- Whitford-Stark, J.L., 1982, A preliminary analysis of lunar extra-mare basalts: Distribution, compositions, ages, volumes, and eruption styles: *The Moon and the Planets*, v. 26, p. 323–338.